

Longitudinal Vehicle Controller Design for IVHS Systems

J. K. Hedrick, D. McMahon, V. Narendran and D. Swaroop

Department of Mechanical Engineering
University of California, Berkeley, CA 94720

Abstract

This paper describes a combined throttle/brake control algorithm designed to control intervehicle spacing within a fully automated "platoon" of vehicles. The control algorithm is developed using a modified sliding control method due to the inherent nonlinearities that exist in current automotive vehicles. The controller is designed using a simplified four state vehicle model and then simulated on a more complete nine state model. Simulations are shown for a two vehicle platoon and for a four vehicle platoon. The four vehicle platoon simulations illustrate the need for "feedforward" platoon information to eliminate disturbance amplification within the platoon. It is shown that communicating the lead vehicle's velocity and acceleration to all platoon vehicles is sufficient to prevent this amplification.

1. Introduction

The concept of fully automated vehicles travelling in "electronically coupled" platoons is not a new one (Caudill and Garrard (1977) and Shladover, S. (1978)). Although of some theoretical interest in the early 1970's it has taken the severe traffic near around major urban centers in the late 1980's to rekindle interest around the world.

As part of the PATH program (Program for the Advanced Technology Highway) at the University of California at Berkeley (Shladover et al. (1990)), the authors have been developing longitudinal control algorithms for close intervehicle spacing within platoons. The basic vehicle and engine modeling is presented in Cho and Hedrick (1989) and Moskwa & Hedrick (1990). A summary of the modeling and preliminary throttle control algorithms are presented in McMahon, Hedrick & Shladover (1990).

In this paper we develop a modified longitudinal control algorithm as well as the logic required to switch between throttle and brake pressure control.

2. Simplified Vehicle Model for Control

This section develops a simplified four state longitudinal powertrain model for control system design. The developed controller is then simulated on a more complete model described in Cho and Hedrick (1989).

The the flow of air into and out of the intake manifold is described by:

$$\dot{m}_a = \dot{m}_i - \dot{m}_c \quad (1)$$

where m_a is the mass of air in the intake manifold and \dot{m}_i and \dot{m}_c are the mass flow rates through the throttle valve and into the cylinders, respectively.

Empirical equations developed for these rates (see Cho and Hedrick (1989) for details) are:

$$\dot{m}_i = \max \cdot TC(\alpha)PRI(P_m/P_a) \quad (2)$$

$$\dot{m}_c = c_1 \eta_v(P_m, \omega_e) m_a \omega_e \quad (3)$$

where \max is a constant dependent on the size of the intake manifold, $TC(\alpha)$ is the throttle characteristic which is a nonlinear function of the throttle angle, α , and $PRI(P_m/P_a)$ is the "pressure ratio influence" function which is a nonlinear function of the ratio of the manifold pressure, P_m , and atmospheric pressure, P_a . The PRI function describes the choked flow relationship that often occurs through the throttle valve. In equation (3) c_1 is a constant for a particular engine, η_v is the "volumetric efficiency" which is generally determined by steady-state tests for a given engine. In order to relate P_m and m_a , we will assume that the ideal gas law for air is valid, i.e.,

$$P_m = \frac{\bar{R} T_m}{V_m} m_a \quad (4)$$

where \bar{R} is the universal gas constant for air, T_m is the temperature in the intake manifold and V_m is the volume of the intake manifold.

Next we describe the engine's rotational dynamics by:

$$J^* \dot{\omega}_e = T_{net}(\dot{m}_{a_e}, \omega_e) - T_L \quad (5)$$

T_{net} is the combined combustion and friction torque and is generally measured by steady-state engine tests and supplied in tabular form as a function of the air flow rate into the cylinders (\dot{m}_{a_e}) and the engine RPM, ω_e . We have assumed here that the spark advance is controlled independently and set to produce maximum brake torque. J^* is the effective inertia attached to the engine and T_L is the effective load applied to the engine. For the controller design we have assumed that there is a rigid link between the engine and the driven tires, therefore J^* includes the engine, torque converter, transmission, driveline, and tire inertia all reflected to the engine (note that J^* will thus be a function of the transmission gear ratio). Under these assumptions T_L becomes:

$$T_L = (hF_{tr} + T_{br}) * R^* \quad (6)$$

where R^* accounts for gear ratios between the wheel and the engine, clearly this assumption also provides:

$$\omega_w = R^* \omega_e \quad (7)$$

In equation (6), h represents the effective radius of the driven wheel, F_{tr} is the tractive force due to the slip which is defined as:

$$i = \frac{h\omega_w - V}{h\omega_w} \quad (8)$$

For simplicity we will assume that the longitudinal tractive force is a saturation function of the slip, i.e.,

$$F_{tr} = K_r \text{sat}(i/\bar{i}) \quad (9)$$

where K_r is the longitudinal tire stiffness and \bar{i} depends on the road and tire condition but is usually around .15 (Wong (1990)).

A very simple linear brake actuator model is assumed:

$$\tau_{br} \dot{T}_{br} + T_{br} = P_c(\mu A_r) \quad (10)$$

where τ_{br} is the actuator time constant, T_{br} is the brake torque applied to the driven wheel, P_c is the commanded brake pressure and μA_r are brake pad parameters. We have assumed here that all the braking is done by the driven (rear) wheels. In our simulation we treat this as the total commanded pressure and distribute the pressure between the front and rear brakes.

Finally we have the longitudinal equation for the

vehicle:

$$M\dot{V} = F_{tr} - cV^2 - F_{rr} \quad (11)$$

where V is the vehicle velocity, cV^2 is the aerodynamic drag and $F_{rr} = \mu Mg$ is the rolling resistance.

3. Nonlinear Controller Design

Due to the severe nonlinearities in the engine and powertrain dynamics, a nonlinear controller design method called the "sliding control" method was used [Moskwa and Hedrick (1990), Green and Hedrick (1990), McMahon, Hedrick and Shladover (1990)]. We will also utilize the "multiple surface" approach [Green and Hedrick (1990), McMahon, Hedrick and Shladover (1990)] developed for systems with nondifferentiable nonlinearities.

Figure 1 illustrates the spacing in a platoon with an arbitrary number of vehicles. The distance, $L_i(t)$, between the i^{th} and $i-1^{\text{th}}$ vehicle is:

$$L_i(t) = x_{i-1} - x_i - d_i - d_{i-1} \quad (12)$$

where x represents an inertial position of the c.g. of the vehicle and d represents fixed vehicle geometry. $L_i(t)$ represents the spacing between the i^{th} and $i-1^{\text{th}}$ vehicles and could be either a constant (e.g. 1 m) during constant speed operation or a time-varying function during vehicle entry or exit. We next define the spacing error, ϵ_i , as:

$$\epsilon_i = x_i - x_{i-1} + L_{i_d}(t) + d_i + d_{i-1} \quad (13)$$

where $L_{i_d}(t)$ represents the desired spacing between the two vehicle. Next following the multiple surface sliding control methodology (McMahon, Hedrick and Shladover, 1990) we define the first surface to be:

$$S_1 = \dot{\epsilon}_1 + c_1 \epsilon_1 + c_2 \int_0^t \epsilon_1 dt \quad (14)$$

which when differentiated yields:

$$\dot{S}_1 = \ddot{\epsilon}_1 - \ddot{a}_{i-1} + c_1 \dot{\epsilon}_1 + c_2 \epsilon_1 \quad (15)$$

Since we have no control in equation (15), we define a "synthetic output" such that

$$\dot{S}_{1_{des}} = -K_1 S_1 \quad (16)$$

using equations (8), (11) and (16) yields:

$$i_{des} \triangleq \frac{m}{K_r} \left(\frac{cV^2}{m} + F_{rr} + \ddot{a}_{i-1} - c_1 \dot{\epsilon}_1 - c_2 \epsilon_1 - K_1 S_1 \right) \quad (17)$$

Substituting (17) into (15) yields:

$$\dot{S}_1 = \frac{K_r}{m} (i - i_{\text{des}}) + \delta f_1 - K_1 S_1 \quad (18)$$

where δf_1 represents modelling errors associated with equation (11). K_1 must be chosen so that $S_1 \dot{S}_1 < 0$ outside of a region defined by $|S_1| < \phi_1$. ϕ_1 is a tracking accuracy design parameter. By using equations (7) and (8) we can define a desired engine speed, i.e.,

$$\omega_{e_{\text{des}}} = \frac{V}{R^*(1-i_{\text{des}})h} \quad (19)$$

At this point we define a second surface, S_2 ,

$$S_2 \triangleq \omega_e - \omega_{e_{\text{des}}} \quad (20)$$

By following a similar procedure as in equations (16)-(19) we obtain

$$T_{\text{net}}(m_{a_{\text{des}}}, \omega_e) = T_L(\omega_e, V) + J^*(\dot{\omega}_{e_{\text{des}}} - K_2 S_2)$$

Equation (21) defines $m_{a_{\text{des}}}$ (or using equation (4), $P_{m_{\text{des}}}$). In general steady-state engine maps stored in table lookup form can be quickly solved for $m_{a_{\text{des}}}$ once the right-hand side of equation (21) is specified. Substituting equation (21) into the S_2 equation yields.

$$\dot{S}_2 = \frac{1}{J^*} (T_{\text{net}} - T_{\text{net}_{\text{des}}}) + \delta f_2 - K_2 S_2 \quad (22)$$

where δf_2 represents the model error in equation (5), thus K_2 must be chosen large enough so that $S_2 \dot{S}_2 < 0$ for $|S_2| > \phi_2$.

Finally we define a third surface, S_3 ,

$$S_3 \triangleq m_a - m_{a_{\text{des}}} \quad (23)$$

and

$$\dot{S}_3 = \dot{m}_a - \dot{m}_{a_{\text{des}}} \quad (24)$$

Using equations (1), (2) and (3) yields

$$\dot{S}_3 = \dot{m}_a - \dot{m}_{a_e} - \dot{m}_{a_{\text{des}}} \triangleq -K_3 S_3 \quad (25)$$

Solving for TC (α) yields

$$TC(\alpha) = \frac{(\dot{m}_{a_e}(m_a, \omega_e) + \dot{m}_{a_{\text{des}}} - (K_3 S_3))}{(MAX \cdot PRI(P_m/P_a))} \quad (26)$$

Equation (26) can be inverted to find the desired throttle angle α . If the resulting angle is negative, then braking is required and we need to return to equation (6) with $T_{br} \neq 0$. Since during braking both the rear and front wheel brakes are used we need to modify equation (11), i.e.,

$$m\dot{V} = F_{tr} + F_{fr} - cV^2 - F_{rr} \quad (27)$$

where

$$F_{tr} = K_r \text{sat}(i_r \bar{f}) \quad (28)$$

$$F_{fr} = K_r \text{sat}(i_r \bar{f})$$

Our strategy will be to solve for the rear brake pressure as the control variable and then to command a total brake pressure that accounts for the distribution of brake pressure front to rear. This leads to

$$i_r \triangleq \frac{m}{K_r} \left[\frac{-K_r \dot{i}_r}{m} + \bar{\mu} Tg + \frac{cV^2}{m} + a_{i-1} - c_1 \dot{\epsilon} - c_2 \epsilon - K_1 S_1 \right] \quad (29)$$

Equation (20) repeated is:

$$S_2 \triangleq \omega_e - \omega_{e_{\text{des}}} \quad (30)$$

$$\dot{S}_2 = \frac{1}{J^*} (T_{\text{net}} - R^* T_{br} - R^* h F_{tr} + R^* h \bar{\mu} mg) - \dot{\omega}_{e_{\text{des}}}$$

Setting

$$\dot{S}_2 = -K_2 S_2$$

yields

$$T_{br_{\text{des}}} = \frac{1}{R^*} [J^*(K_2 S_2 - \dot{\omega}_{e_{\text{des}}}) + T_{\text{net}} - h(K_r i_r - \bar{\mu} mg)] \quad (31)$$

Next we define

$$S_4 \triangleq T_{br} - T_{br_{\text{des}}} \quad (32)$$

$\dot{S}_4 \triangleq -K_4 S_4$ yields

$$P_c = \frac{1}{\mu A r} [\tau(\dot{T}_{br_{\text{des}}} - K_4 S_4) + T_{br}] \quad (33)$$

Assuming a 60-40 split, front to rear, then the total commanded pressure would be $P_{c_r} = 2.5 P_c$.

4. Simulations

2 car platoon. The first simulations were performed by considering a single vehicle under closed-loop control tracking a lead vehicle whose velocity is a specified function of time. The simulation as outlined in McMahon & Hedrick (1990), includes a torque converter model, drive axle compliance and front and rear wheel rotational degrees of freedom. The engine model also has time delays due to combustion transport phenomena. The vehicle parameters utilized in the simulation were for a typical passenger car and are similar to those in

McMahon, Hedrick & Shladover (1990).

For the computer implementation the terms $\dot{\omega}_{a_{i-1}}$, $\dot{m}_{a_{i-1}}$, and $T_{br_{i-1}}$ were all computed numerically using a first order finite difference.

Figure 2 shows the results of the rear vehicle following a typical change of velocity profile. The tracking accuracy is quite good with the maximum spacing error of 4 cm (1 m is the nominal spacing).

4 car platoon. Next a four car platoon (three following vehicles under closed-loop control tracking a lead vehicle with a specified velocity profile) Figure 3 shows the results with the vehicles using the control algorithm defined by equations (13)-(33). The tracking results look quite reasonable; however, a disturbing trend is shown in Figure 3(b), i.e., each vehicle's peak error is amplified as one goes rearward in the platoon. In a large platoon (≈ 20 vehicles) this would result in large gaps during acceleration and potential crashes during braking.

This problem of error amplification in platoons has been observed in the literature and can be alleviated by communicating additional vehicle information to all vehicles within the platoon. A simple way to achieve this within the context of sliding control is to redefine equation (14) as:

$$S_1 \triangleq \dot{\epsilon}_1 + c_1 \epsilon_1 + c_2 \int \epsilon_1 dt + c_3 (V_1 - V_l) \quad (34)$$

where V_l is the velocity of the lead vehicle. To see why this is a reasonable approach we can set $\dot{S}_1 = 0$ and see that this implies:

$$\ddot{\epsilon}_1 + \frac{c_1}{1+c_3} \dot{\epsilon}_1 + \frac{c_2 \epsilon_1}{1+c_3} = \frac{c_3}{1+c_3} (a_l - a_{i-1}) \quad (35)$$

In order to achieve similar transient performance as in the previous case we need to redefine c_1, c_2 to include the effect of c_3 . Equation (35) shows that a_l is a feedforward type of input to the error equation and that the forcing term $a_l - a_{i-1}$ will go to zero, as each vehicle in the platoon operates on a similar equation.

Figure 4 shows how the introduction of lead information has resulted in vehicle to vehicle attenuation rather than amplification.

5. Conclusions

A fully nonlinear longitudinal vehicle control algo-

rithm has been developed and simulated on multiple vehicle platoons. The combined throttle/brake algorithm utilizes a multiple surface sliding control method that avoids the need to compute multiple derivatives of an uncertain model.

It was shown how the communication of lead information about the first vehicle's velocity and acceleration to all of the trailing vehicles can eliminate vehicle to vehicle disturbance amplification.

Acknowledgment

This work is part of the Program on Advanced Technology for the Highway (PATH), prepared under the sponsorship of CALTRANS. The authors also wish to thank VORAD, Ford and Ready Systems for their support.

References

- Caudill, R. J., and Garrard, W. L., "Vehicle-Follower Longitudinal Control for Automated Transit Vehicles," *Trans. ASME, JDSM&C*, Vol. 99, No. 4, Dec. 1977.
- Cho, D., and Hedrick, J. K., "Automotive Powertrain Modelling for Control," *Trans. ASME, JDSM&C*, Vol. 111, No. 4, Dec. 1989.
- Green, J. H., and Hedrick, J. K., "Nonlinear Speed Control for Automotive Engines," *Proceedings of the 1990 ACC*, San Diego, CA, May 1990.
- McMahon, D., Hedrick, J. K., and Shladover, S. E., "Vehicle Modelling and Control for Automated Highway Systems," *Proceedings of the 1990 ACC*, San Diego, CA, May 1990.
- Moskwa, J. J., and Hedrick, J. K., "Nonlinear Algorithms for Automotive Engine Control," *IEEE Control Systems Magazine*, April 1990.
- Shladover, S., et al., "Automated Vehicle Control Developments in the PATH Program," *IEEE Trans. on Vehicular Technology*, Feb. 1991.
- Shladover, S., "Dynamic Entrainment of Automated Guideway Transit Vehicles," *High Speed Ground Transportation Journal*, Vol. 12, No. 3, Fall 1978, pp. 87-113.
- Wong, J., *Theory of Ground Vehicles*, J. Wiley, 1979.

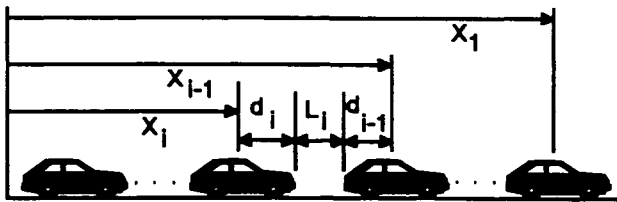


Figure 1. Platoon Spacing

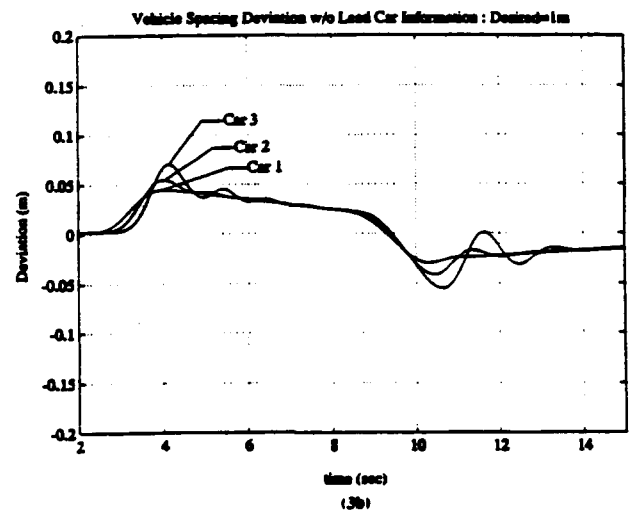
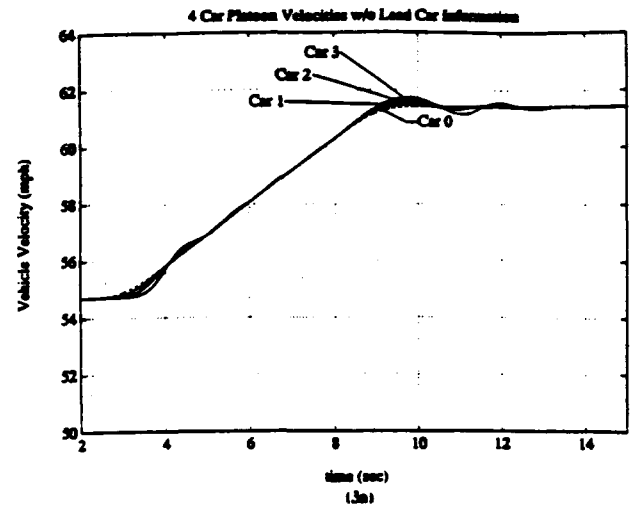


Figure 3. 4-car Platoon Without Lead Information

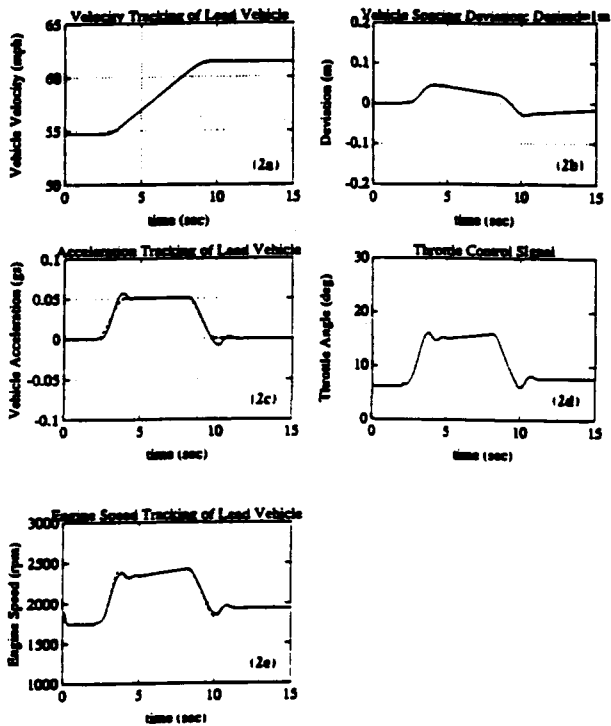


Figure 2. 2-car Platoon

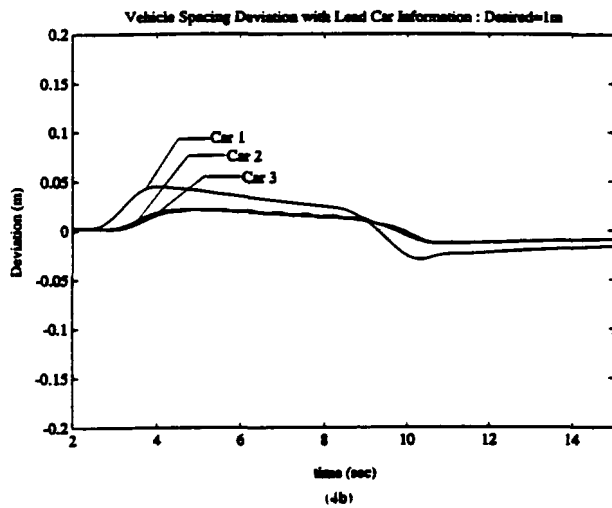
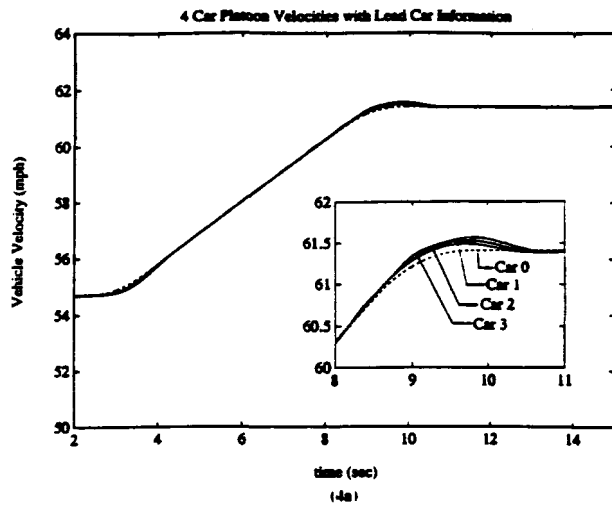


Figure 4. 4-car Platoon With Lead Information